

Responses of a Looming-Sensitive Neuron to Compound and Paired Object Approaches

Bruce B. Guest and John R. Gray

Department of Biology, University of Saskatchewan, Saskatoon, Saskatchewan, Canada

Submitted 3 October 2005; accepted in final form 25 November 2005

Guest, Bruce B. and John R. Gray. Responses of a looming sensitive neuron to compound and paired object approaches. *J Neurophysiol* 95: 1428–1441, 2006. First published November 30, 2005; doi:10.1152/jn.01037.2005. The lobula giant movement detector (LGMD) and its target neuron, the descending contralateral movement detector (DCMD), constitute a motion-sensitive pathway in the locust visual system that responds preferentially to objects approaching on a collision course. LGMD receptive field properties, anisotropic distribution of local retinotopic inputs across the visual field, and localized habituation to repeated stimuli suggest that this pathway should be sensitive to approaches of individual objects within a complex visual scene. We presented locusts with compound looming objects while recording from the DCMD to test the effects of nonuniform edge expansion on looming responses. We also presented paired objects approaching from different regions of the visual field at nonoverlapping, closely timed and simultaneous approach intervals to study DCMD responses to multiple looming stimuli. We found that looming compound objects evoked characteristic responses in the DCMD and that the time of peak firing was consistent with predicted values based on a weighted ratio of the half size of each distinct object edge and the absolute approach velocity. We also found that the azimuthal position and interval of paired approaches affected DCMD firing properties and that DCMDs responded to individual objects approaching within 106 ms of each other. Moreover, comparisons between individual and paired approaches revealed that overlapping approaches are processed in a strongly sublinear manner. These findings are consistent with biophysical mechanisms that produce nonlinear integration of excitatory and feed-forward inhibitory inputs onto the LGMD that have been shown to underlie responses to looming stimuli.

INTRODUCTION

Effective visually guided collision avoidance behaviors are critical for the survival of many animals (Gibson 1979). Successful execution of these behaviors requires the visual system to be able to extract salient sensory cues related to looming stimuli (objects approaching on a direct collision course). Characterization of looming-sensitive neurons in insects (Hatsopoulos et al. 1995; Simmons and Rind 1992; Wicklein and Strausfeld 2000) and birds (Sun and Frost 1998) have led to studies that provide insights into biophysical mechanisms underlying responses to single approaches of basic shapes (Gabbiani et al. 2002, 2005) or multiple local motion stimuli (Krapp and Gabbiani 2005). In the natural environment, however, animals are often confronted with complex spatiotemporal patterns of visual information. Recent studies based on responses to simplified stimuli have shown that saliency of visual cues is often influenced by emergent properties of complex

visual scenes (see Kayser et al. 2004 for a review). For example, in the monkey inferotemporal cortex, multiple objects may be represented through ubiquitous normalization mechanisms and averaging of summed presynaptic inputs (Zoccolan et al. 2005). However, little is known of how responses of looming-sensitive neurons are influenced by complexity within the visual scene.

Gregarious locusts flying 0.8–9.0 m apart in a swarm (Waloff 1972) are immersed in dynamic, complex visual environments composed of conspecifics and various other objects that move within the visual field. The locust visual system contains a well-defined neural pathway composed of the lobula giant movement detector (LGMD) and its postsynaptic target, the descending contralateral movement detector (DCMD), that is highly responsive to looming stimuli (Hatsopoulos et al. 1995; Judge and Rind 1997; Schlotterer 1977; Simmons and Rind 1992). The three large dendritic fields of the LGMD receive distinct inputs from presynaptic visual afferents (O'Shea and Williams 1974). One of these fields receives excitatory input from many retinotopically arranged fibers that are sensitive to local motion (O'Shea and Rowell 1976), whereas the other two receive local feed-forward inhibition produced by rapid changes in luminance (Rowell et al. 1977). Recent evidence strongly suggests that postsynaptic nonlinear integration of excitatory and feed-forward inhibitory inputs (Gabbiani et al. 2002, 2005; Krapp and Gabbiani 2005) underlie the biophysical mechanisms of looming responses in the LGMD, which is characterized by a firing rate that peaks after a certain retinal threshold angle is exceeded (Gabbiani et al. 1999, 2001, 2002; Matheson et al. 2004). LGMD spikes are transferred to the DCMD in a 1:1 manner (O'Shea and Rowell 1975a; Rind 1984) via mixed electrical and chemical synapses (Killman et al. 1999; O'Shea and Williams 1974). Subsequently, the DCMD connects to flight interneurons and motorneurons within the thoracic ganglia (Burrows and Rowell 1973; Robertson and Pearson 1983; Simmons 1980). Therefore looming responses in this pathway may have consequences for collision avoidance behaviors that are influenced by the angular threshold size of an approaching object (Hatsopoulos et al. 1995; Robertson and Johnson 1993). Recent recordings of DCMD responses to looming stimuli in tethered flying locusts (Santer et al. 2005) notwithstanding, the role of the LGMD/DCMD pathway in collision avoidance has not yet been explored directly.

Although earlier experiments presented locusts with complex visual scenes (Rind and Simmons 1992) there are no

Address for reprint requests and other correspondence: J. R. Gray, Dept. of Biology, 112 Science Place, University of Saskatchewan, Saskatoon, SK, S7N 5E2, Canada (E-mail: jack.gray@usask.ca).

The costs of publication of this article were defrayed in part by the payment of page charges. The article must therefore be hereby marked "advertisement" in accordance with 18 U.S.C. Section 1734 solely to indicate this fact.

quantitative descriptions of how the LGMD/DCMD pathway responds to approaches of complex or multiple objects in the visual field. Recent findings (Gray 2005) predict that the LGMD should be able to respond to approaches of multiple objects approaching from different trajectories. Therefore we designed experiments to examine the effects of object complexity and number on looming responses in this pathway by recording activity in the DCMD. We found that approaching compound objects evoke characteristic looming responses where the time of peak firing is related to the ratio of object half size and object approach velocity. This latter finding is consistent with previous reports on LGMD encoding properties (Gabbiani et al. 1999). We also found that DCMD responses were affected by the azimuthal position of paired looming discs and that closely timed and simultaneous approaches are summed in a strongly sublinear manner. These latter findings can be explained by the relative timing of feed-forward inhibition onto the LGMD dendritic tree.

METHODS

Animals

Twenty two adult male locusts (*Locusta migratoria* L.) were selected ≥ 3 wk past the imaginal molt from a crowded colony (28–25°C, 12·h:12·h light:dark) maintained at the University of Saskatchewan. Experiments were carried out at room temperature ($\sim 25^\circ\text{C}$).

Preparation

After removal of the legs and wings, a rigid tether was attached to the ventral surface of the thorax using Nexaband SC topical tissue adhesive (WPI, Sarasota, FL). The tethered animal was positioned ventral side up, and small patch of ventral cervical cuticle was removed to expose the underlying paired connectives of the ventral nerve cord between the suboesophageal and prothoracic ganglia. The entire preparation was then transferred to the recording setup (see Gray et al. 2002). DCMD activity was monitored with a bipolar silver wire hook electrode placed around the medial and dorsal surface of the left connective and insulated with a mixture of Vaseline and mineral oil. The preparation was then rotated 180° such that the locust was oriented dorsal-side up with its longitudinal axes orthogonal to the apex of the rear projection screen. The right eye was then aligned with the horizontal and vertical axes of the apex. In this orientation 0° was directly in front of the locust, 180° was directly behind and 90° (the center of the eye) was aligned with the dome apex (see Fig. 1A). The preparation was left for ≥ 30 min in front of a projected white visual field before the experiment started to allow the animal to acclimate to the experimental setup and the background luminance that was used for each approach.

Visual stimuli

Computer-generated objects were created as $1,024 \times 1,024$ -pixel portable network graphics (png) files and scaled in real-time at 85 frames/s (fps) using the Vision Egg visual stimulus generation software (A. Straw; <http://visionegg.org/>) running on a Python programming platform. The maximal distance from the apex of the dome and the edge of a projected looming object was 14 cm (see following text). Within this region, the size of each projected pixel was 0.7 mm, resulting in a visual subtense angle of $\sim 0.4^\circ$, which is below the resolution of individual ommatidia in the acute zone of the eye (1°) (Horridge 1978). Pixels at the edges of the projection area would likely extend beyond the resolution of an individual ommatidium due

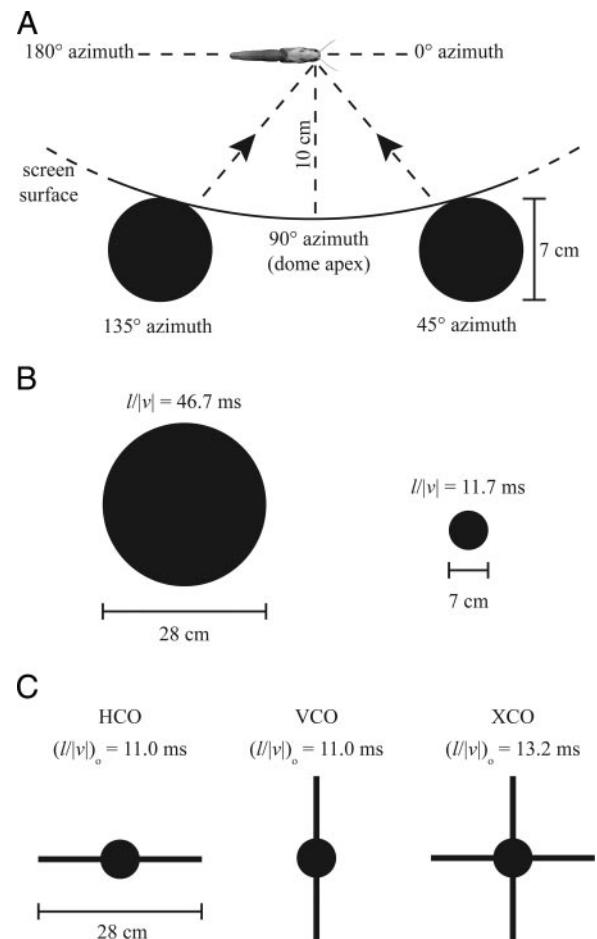


FIG. 1. Computer-generated objects presented to tethered *L. migratoria*. A: expanded view of the dome apex showing the orientation of the locust and the approach angles of the looming 7 cm disks. Paired approaches consisted of 2 disks approaching from 45° and/or 135° at 4 s, 3 s, 0.106 s, or 0 s intervals. Single objects approaching from 90° at 3 ms^{-1} were simple disks [28 or 7 cm diam (B) or compound shapes (C) consisting of a 7 cm central disk with horizontal and/or vertical extensions (see text for details)]. Values of $l/|v|$ (B) or $l/|v|_o$ (C) are indicated above each object.

to distortion by the curvature of the dome. However, these pixels were part of the white background and thus did not affect the resolution of the approaching objects. The scaling factor, adjusted to real-world coordinates, for each frame was calculated to emulate nonlinear edge expansion produced by a looming object. We used a 1.2-ms TTL pulse included in each video frame and the Vsync pulse from the video card (NVIDIA GeForce4 Ti4200 128 MB) to align the DCMD recordings with the time of collision. The frame at which the object disappeared from the screen was identified by the last TTL pulse, and the start time of the rendering of this frame was determined by the corresponding Vsync pulse. The frequency of the TTL and Vsync pulses also confirmed the frame rate throughout each approach. Images were projected onto the convex surface of a rear projection dome screen at 85 fps using a Sony VPL-PX11 LCD data projector. Correction factors were embedded in the Vision Egg code to account for distortion due to projection onto the curved surface of the screen. The luminance values and Michelson contrast ratio (0.48) were the same as those used by Gray (2005). All looming objects were presented at 0° elevation, i.e., within the azimuthal plane.

To test for effects of looming object shape on DCMD firing, we used either simple black disks (diameter = 28 or 7 cm, Fig. 1B) or compound shapes consisting of disks (diameter = 7 cm) with bilateral extensions (10.5 cm L x 1.2 cm W) oriented horizontally (designated

HCO for horizontally oriented compound object), vertically (VCO), or both (XCO). The total compound object width and/or height was 28 cm (Fig. 1C). HCO was used to replicate the looming bird profile used by Gray (2005), and VCO and XCO were used to test different orientations and numbers of extensions that represent different levels of object complexity. Simple looming objects such as squares or disks are defined by uniform expansion of the edge throughout approach, which is determined by the ratio of the half size of the object (l) and the absolute value of the approach velocity ($|v|$), i.e., $l/|v|$. Edges of compound objects, however, expand nonuniformly during approach and thus a single value of $l/|v|$ does not describe expansion parameters of the entire object. Therefore we calculated the mean weighted value of $l/|v|$ for each compound object as

$$\left(\frac{l}{|v|}\right)_o = \sum_{i=1}^n \left(\frac{l}{|v|}\right)_i P_i \quad (1)$$

where n is the number of unique edges ($n = 3$ for the compound objects used here) and P_i is the proportion of the object perimeter occupied by each unique edge type. The weighted values for the compound objects we used are: HCO and VCO = 11 ms and XCO = 13 ms. These values are close to the $l/|v|$ value of the 7-cm disk (12 ms) and lower than that of the 28-cm disk (47 ms) and predict that DCMD firing properties during approaches of the compound objects should be similar to those during approaches of a 7-cm disk. We did not include expansion at the corners of the tips of the horizontal and vertical projections in the compound objects because corners of a looming square contribute little to the firing properties of the LGMD (Gabbiani et al. 2001).

Each single simple and compound object approached from 20 m away at 3 m/s on a direct collision course from 90°, producing an approach duration of 6.67 s. The respective initial and final subtense angles for each object were 0.8 and 109° (28-cm disk and extensions of compound objects) and 0.2 and 39° (7-cm disk and central disc of compound objects). Each object remained on the screen for 1 s after the end of approach to avoid confounding effects of a DCMD OFF response (see following text). Thus each sequence, including approach and retention time, lasted 7.67 s.

To test for effects of multiple approaches on DCMD firing, we presented pairs of 7-cm-diam disks approaching at 3 m/s from 45 or 135° at four different start intervals (Fig. 1A). These two approach angles were chosen because at the end of approach the adjacent edges of each disk were 14 cm apart along an arc centered at the dome apex. At this distance and accounting for the distance between the locust's eye and points along the arc, the disks were separated by 70° of the visual field. Therefore each disk would stimulate a different ommatidial array. Given that each ommatidium has a spatial resolution of 1–1.25° (Horridge 1978) and a light-adapted acceptance angle of 1.5° (Wilson 1975), we avoided potential confounds due to repeated stimulation and habituation of synaptic inputs onto the LGMD (Gray 2005; Matheson et al. 2004). Each 3-s approach started from 9 m away, producing initial and final subtense angles of 0.4 and 39°, respectively, for each disk. The intervals between the start of approach for each object were 4, 3, 0.106, and 0 s (simultaneous approach) producing respective sequence durations of 8, 7, 4.106, and 4 s. Pairs approaching at 3 m/s with an interval of 0.106 s have an approach distance difference of 31.8 cm. When the first object passed through a subtense angle of 10°, which is known to evoke collision avoidance maneuvers in tethered flying locusts (Robertson and Johnson 1993), the second object would subtend 6° of the field of view. When the second object reached 10°, the first object would still be 8.2 cm (27 ms) from collision. Therefore this interval was used to examine whether the DCMD was able to respond to a second object that passed through a behaviorally relevant subtense angle, while the first object, having already passed through the same angle, was still approaching. For objects approaching with a 3-s interval, the first object remained

on the screen throughout the second approach. Both objects disappeared 1 s after the end of the second approach. For objects approaching with a 4-s interval, the start of approach of the second object corresponded to the disappearance of the first object (i.e., 1 s after the 1st object stopped approaching). The 3-s and 4-s approach intervals were designed to test whether the continued presence of the first object affected the response of the DCMD to the second object. We presented each paired interval twice, reversing the order of the first approach angle (i.e., 45° first or 135° first). Including all combinations of single and paired objects, each locust was presented, in random order, with 12 unique approaches (i.e., 1 approach for each condition). To avoid habituation to approach sequences, we gently brushed the locust's abdomen at the end of each trial and then waited ≥ 5 min before the start of the next approach sequence.

DCMD activity

Continuously recorded activity from the left cervical connective was amplified with a differential AC amplifier (A-M Systems, model No. 1700, gain = 1,000), sampled at 25 kHz and stored to disk using a RP2.1 enhanced real-time processor (Tucker-Davis Technologies, Alachua, FL) with Butterworth filter settings of 100 Hz (high pass) and 5 kHz (low-pass). An additional data channel was used to record the 1.2-ms TTL pulses that were synchronized with each frame of the stimulus playback. These pulses were used to align the Vsync pulses from the video card and thus determine the time of the last presentation frame (see preceding text). This time was used to calculate the projected time of collision.

We used threshold values set up in Off-line Sorter (Plexon, Dallas, TX) to identify DCMD spikes in each data stream from the cervical connective. DCMD activity was readily identified by the large-amplitude spikes in the connective that responded to looming stimuli. Spike times were transformed into instantaneous spike rates and smoothed with a 50-ms Gaussian filter using Neuroexplorer spike train analysis software (NEX Technologies, Littleton MA). We quantified DCMD activity by measuring, for each approach, the time of the peak firing rate relative to collision, the amplitude of the peak, the number of spikes from $t = -3$ to 0.5 s relative to collision and the spike rate 200 ms before collision (Fig. 2A) (see also Gray 2005). We measured additional parameters for different combinations of paired approaches. For paired approaches at 4- and 3-s intervals, we measured the number of spikes and the spike rate 200 ms before collision for both approaches, whereas for the 0.106-s interval, these parameters were measured relative to the first projected collision only. For single approaches and paired approaches at 4-, 3-, and 0-s intervals, we measured the width of the smoothed response at half the peak amplitude as an estimation of peak duration. For paired approaches at an interval of 0.106 s, we measured the time between the two peaks, the spike rate at the valley between the two peaks, the time of the valley relative to the second collision (Fig. 2B), and the number of spikes from the valley or the first collision to 0.5 s after the second collision. Two distinct peaks at this interval precluded us from estimating the duration of a single peak. Therefore we measured the duration between the rising phase of the first peak and the falling phase of the second peak at one half the maximal spike rate.

Statistics

Data were plotted using SigmaPlot 9.0, and statistical tests were performed using SigmaStat 3.1. Effects of object shape, approach angle, or approach interval were tested using a one-way ANOVA (Kruskal Wallis ANOVA on ranks for nonparametric data) or Student's t -test (Mann-Whitney rank sum test for nonparametric data). Data that showed significant effects from ANOVA were further compared using a Holm-Sidak (Dunn's for nonparametric data) multiple comparison. Significance was assessed at $P < 0.05$.

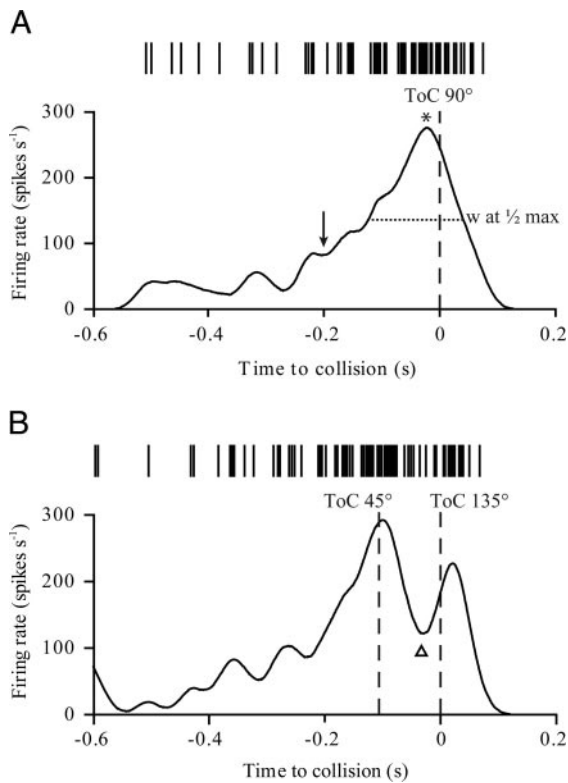


FIG. 2. Quantification of descending contralateral movement detector (DCMD) firing parameters during approach. Time-aligned raster plot (*top*) and Gaussian smoothed instantaneous firing rate (*bottom*) from a single representative approach of a 7-cm disk from 90° (A) or paired approaches at 0.106-s intervals (B). For single approaches (A) and 2 objects approaching at 4- and 3-s intervals (not shown), we measured the amplitude and time, relative to collision, of the peak firing rate (*), the duration of the peak at half peak amplitude (w at 1/2 max), the instantaneous firing rate 200 ms before collision (\downarrow) and the number of spikes during approach. Paired approaches 0.106 s apart (B) produced 2 distinct peaks that were delimited by a decreased firing rate (valley, Δ). See text for a description of quantitative measures of the response. ToC, time of collision (- - -). The peristimulus time histogram in B was aligned with the time of 2nd collision.

RESULTS

DCMD responses to looming objects

The DCMD responded to approaching objects with an increasing spike rate that reached a peak near the time of predicted collision (Figs. 2 and 3). For all stimulus types used, the responses were remarkably consistent between animals (rasters showing single trials per animal and peristimulus histograms in Fig. 3). Typical of DCMD looming responses (Gabbiani et al. 1999; Gray et al. 2001; Rind and Simmons 1992), approaches of the larger (28 cm) disk ($|v| = 47$ ms) resulted in a relatively slow increase in spike rate that peaked ~ 100 ms before collision, whereas the response to the smaller (7 cm) disk ($|v| = 12$ ms) was of shorter duration and peaked closer to collision (Fig. 3A).

Responses to compound objects

The amplitude and time of the peak in response to compound objects were similar to those for a 7-cm disk, whereas earlier in the response there were subtle, orientation-dependent, differences. Whereas HCO (Fig. 3B) and VCO (Fig. 3C) produced a response that was similar to that from a 7-cm disk, responses to

XCO consistently displayed a small early peak that occurred 200 ms before collision (Fig. 3D, arrow). For all single approaches, there were clear differences in the DCMD firing parameters measured, especially between a 28-cm disk and all other single objects (Fig. 4). There was a significant difference in the peak firing rate among the different object types [1-way ANOVA, $F(4,104) = 10.8$, $P < 0.001$]. The peak firing rate in response to a 28-cm disk was lower than for a 7-cm disk, VCO, and XCO, but was not significantly different from that of HCO (Fig. 4A). However, at $\alpha = 0.05$, the power of a separate t -test (0.265) between a 28-cm disk and HCO is low, and so this similarity should be interpreted with caution. Interestingly, there was no difference in the peak firing rate between a 7-cm disk and all compound objects, whereas between different compound objects, the peak during approaches of HCO were smaller than for VCO but similar to XCO. There was also a significant effect of object type on the peak firing time (Fig. 4B, Kruskal-Wallis ANOVA on ranks, $H_4 = 54.0$, $P < 0.001$), the peak duration (Fig. 4C, $H_4 = 54.7$, $P < 0.001$), the firing rate 200 ms before collision [Fig. 4D, $F(4,104) = 87.1$, $P < 0.001$], and the number of spikes [Fig. 4E, $F(4,104) = 38.7$, $P < 0.001$]. Peak firing occurred significantly earlier and the peak duration was significantly longer (Fig. 4C) for approaches of a 28-cm disk but was invariant for all remaining objects. The spike rate 200 ms before collision and the number of spikes during approach were greatest for a 28-cm disk, whereas XCO produced intermediate values that were greater than during approaches of the other objects. These results suggest that the peak firing rate, time, and duration were affected by object size but were relatively insensitive to object shape. Shape did, however, influence the spike rate 200 ms before collision and the total number of spikes (Fig. 4, D and E).

As predicted by the values of $(|v|)_0$ and the clustering shown in Fig. 5, the compound objects used here generated peak times that were very close to those generated by approaches of a 7-cm disk. We used a linear regression through these data to obtain estimates of the threshold angle (θ_{thresh}) and its associated delay (δ), which are parameters that relate DCMD firing properties to the approaching stimulus (see Gabbiani et al. 1999 for derivation). These estimates showed that the peak spike rate occurred 20.2 ± 15.0 ms (mean \pm SD) after the stimulus reached a threshold angle of $41.5 \pm 15.4^\circ$.

Responses to simultaneously approaching object pairs

Recent findings strongly suggest that the LGMD performs a multiplicative operation based on excitation and feedforward inhibition to encode the approach of a looming object (Gabbiani et al. 2002, 2005). Thus it is likely that nonlinear processes also control responses to multiple looming objects. Simultaneous approaches affected the peak firing rate [$F(3,82) = 287.3$, $P < 0.001$], the firing rate 200 ms before collision [$F(3,82) = 34.4$, $P < 0.001$], and the number of spikes [$H_3 = 60.5$, $P < 0.001$]. Generally, responses to simultaneously approaching 7-cm disks from 45 and 135° were stronger than responses to approaches from each angle individually but dramatically weaker than a predicted linear sum of the two responses (Fig. 6A).

The peak firing rate was higher during individual approaches from 135° than for approaches from 45° which, in turn, were both lower than for simultaneous approaches from both angles

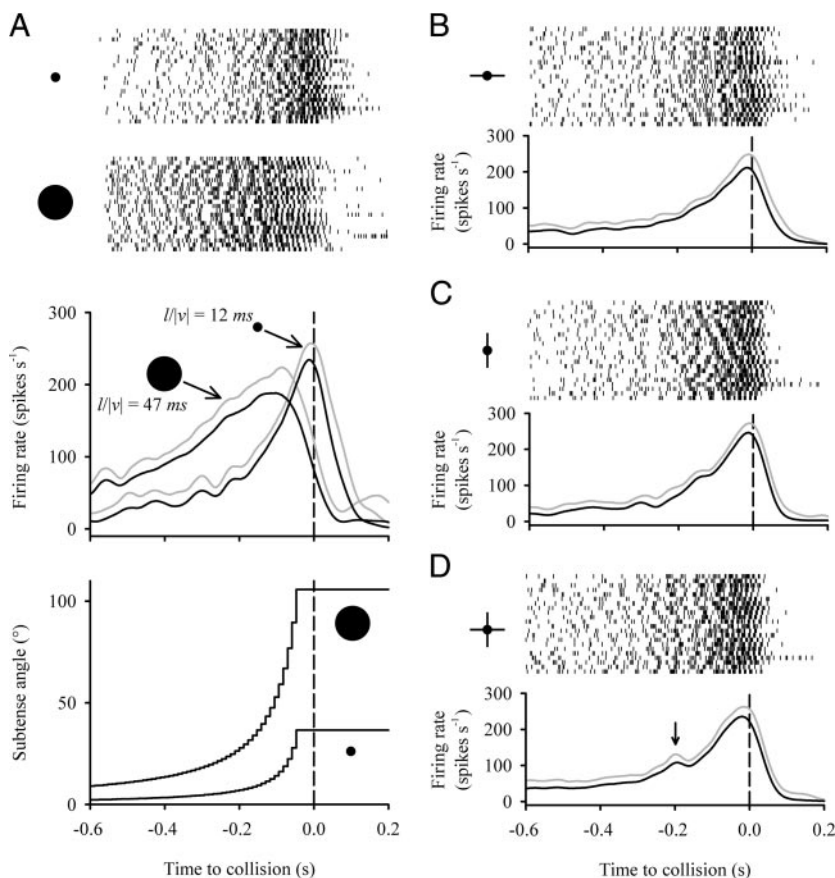


FIG. 3. DCMD responses to simple and compound looming objects. *A*: raster plots of spike times aligned to time of collision during approaches of a 7-cm (*top*) or 28-cm (*bottom*) disk. Mean (black line) and positive SD (gray line) of Gaussian-smoothed instantaneous spike rates during approaches. *Bottom*: increasing angle of visual subtense for each simple object during approach. *B–D*: raster plots (*top*) and smoothed instantaneous firing rates (*bottom*) of responses to compound objects. The arrow in *D* indicates a small early peak of the firing rate during approaches of a horizontally and vertically oriented compound object (XCO, see text for designation of compound objects). Each raster line represents data from 1 animal ($n = 22$).

(Fig. 6*B*). The peak firing rate in response to simultaneous approaches, however, was significantly lower than the predicted linear sum. The timing of the peak (Fig. 6*C*) was unaffected by approach angle, simultaneous approaches, or a predicted linear sum of individual approaches. Similarly, peak duration was unaffected by approach angle or simultaneous approaches, which were both significantly lower than a linear sum (Fig. 6*D*). Single approaches from 135° produced the lowest spike rate 200 ms before collision whereas individual approaches from 45° and simultaneous approaches produced similar spike rates at this time (Fig. 6*E*). The linear sum of this parameter was significantly higher than for the other conditions. Individual approaches resulted in a similar number of spikes throughout the approach that was lower than during simultaneous approaches, which were also summed sublinearly (Fig. 6*F*).

These results predict that DCMD responses to simultaneous approaches should be similar to responses to a 7-cm disk approaching from 90° even though the distance between the outer edges of the paired disks matched the diameter of the 28-cm disk approaching from 90°. Therefore we compared DCMD firing parameters between individual approaches of each disk size from 90° and paired approaches using a one-way ANOVA followed by a Holm-Sidak multiple comparison. We found that responses to simultaneous approaches were almost identical to responses evoked by approaches of a 7-cm disk from 90° (compare the solid black lines in Fig. 6*A* with the response to a 7-cm disk in Fig. 3*A*, *middle*). The only significant difference was a higher peak firing rate for simultaneous approaches [$F(2,63) = 27.5$, $P < 0.001$]. The differences

between simultaneous approaches and approaches of a 28-cm disk were the same as those between the two disk sizes approaching from 90° (see Figs. 3 and 4). In accordance with previous findings (Krapp and Gabbiani 2005), these results demonstrate that LGMD processing of simultaneous, nonoverlapping approaches is strongly sublinear.

Effects of approach interval on DCMD responses to looming

For 4- and 3-s approach intervals, the response profiles were similar and appear to depend on the approach angle (Fig. 7, *A–D*). Irrespective of approach order, approaches from 45° appear to produce a lower peak firing rate than approaches from 135°. Approaches 0.106 s apart from either initial angle produced two distinct peaks in the firing rate (Fig. 7, *E* and *F*). The first peak occurred close to the time of first collision, whereas the second peak occurred slightly after the second collision (see arrows in Fig. 7, *E* and *F*). The two peaks were more distinct for initial approaches from 45° than from 135° due to a more pronounced decrease in the firing rate (valley, open arrowheads) between the two times of collision. To assess whether DCMD responses were sensitive to changes in approach angles that deviated from 90° and if sensitivity was affected by the approach interval, we compared parameters of the response centered around the first approach (4- and 3-s intervals) to those of single approaches of a 7-cm disk from 90° (Fig. 8, *A*, *C*, *E*, *G*, and *I*). Although the peak firing rate was unaffected by the approach angle or the interval (Fig. 8*A*), it occurred significantly later for approaches that deviated from 90°, irrespective of the interval [Fig. 8*C*, $F(6,146) = 6.04$, $P <$

0.001]. Because the response to the second approach was masked by the response to an approach 0.106 s earlier (see Fig. 7, *E* and *F*), we measured the entire response at half the peak firing rate and the firing rate 200 ms before the first collision for approaches at 0.106-s intervals. Compared with approaches

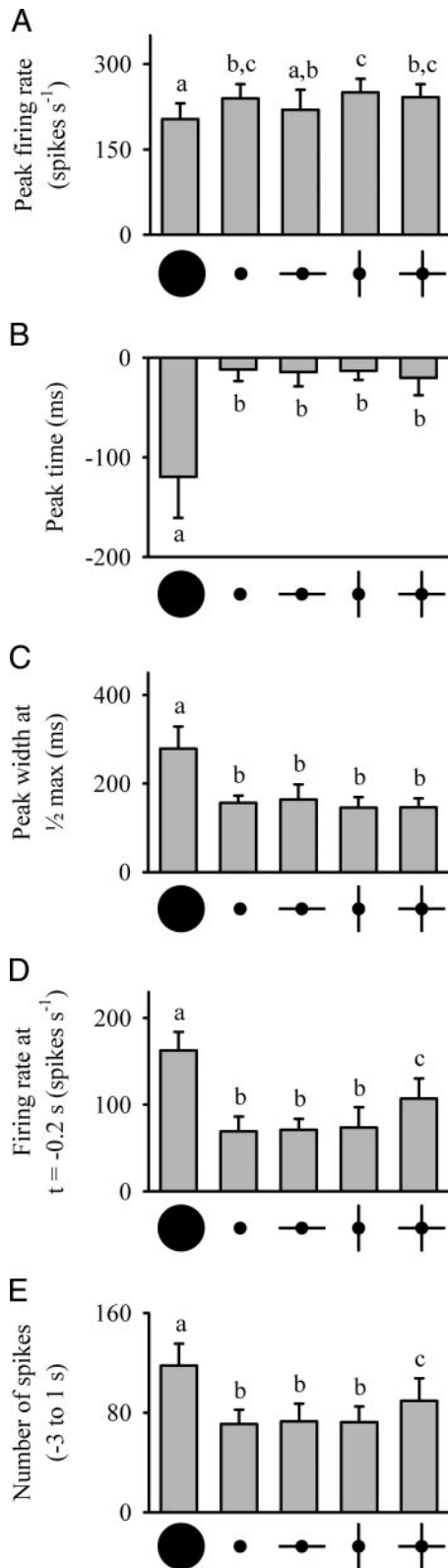


FIG. 5. The linear relationship between $(l/|v|)_0$ and peak firing time during approach was maintained for simple (●) and compound objects (○). The equation of the line was used to calculate values of the threshold angle (θ_{thresh}) and its associated delay (δ) (see text). Note that the data points for HCO and VCO overlap at the lowest $(l/|v|)_0$ values. Data represent the means \pm SD, $n = 22$.

from 90°, the peak duration was significantly shorter for 4- and 3-s approach intervals, and the entire response duration was significantly longer for 0.106-s intervals. Comparing between angles for all paired approaches, the response duration was shorter for approaches from 135° (Fig. 8*E*). The firing rate 200 ms before collision was also affected by approaches that deviated from 90° [$F(6,146) = 5.0$, $P < 0.001$] and was significantly lower for all approaches from 45 and 135°, irrespective of the approach interval (Fig. 8*G*). Initial approaches from either angle at 4- and 3-s intervals and from 135° at 0.106-s intervals evoked fewer spikes than approaches from 90° [Fig. 8*I*, $F(6,146) = 25.3$, $P < 0.001$]. These data suggest that although the peak firing rate was insensitive to changes in approach angle or interval, approaches deviating from 90° resulted in delayed peak firing and decreases in early firing rates and the response duration.

To examine the effects of a looming object on DCMD responses to a second object, we normalized peak amplitude, peak duration, the spike rate 200 ms before collision, and spike number values from the second approach to those of a first approach from the same angle (Fig. 8, *B*, *F*, *H*, and *J*). The time of the second peak was measured relative to the second collision (Fig. 8*D*). There was a significant effect of the approach angle and the approach interval on the peak firing rate ($H_6 = 83.2$, $P < 0.001$), the time of the peak ($H_6 = 54.4$, $P < 0.001$), and the number of spikes ($H_4 = 39.4$, $P < 0.001$). There was no effect on the peak duration (Fig. 8*F*) or the firing rate 200 ms before collision (Fig. 8*H*). The only difference in firing parameters for 4- and 3-s interval data was a significant

FIG. 4. DCMD firing parameters during approaches of simple and compound looming objects. There were significant, though slight, differences in the peak firing rate (*A*) between simple and compound objects. The peak rate was lower for a 28-cm disk than for all other objects except for a horizontally oriented compound object (HCO), and there were no differences in the peak firing rate between a 7-cm disk and all compound objects. The time of the peak (*B*) occurred earlier and the peak width at 1/2 max (*C*) was greater during approaches of a 28-cm disk. There were no significant differences in these 2 parameters between a 7-cm disk and the compound objects. The firing rate 200 ms before collision (*D*) and the number of spikes (*E*) was highest for a 28-cm disk, lowest for a 7-cm disk, HCO and VCO and intermediate for XCO. Data represent the means \pm SD, $n = 22$. Bars with the same letters were not significantly different (see text for statistical parameters).

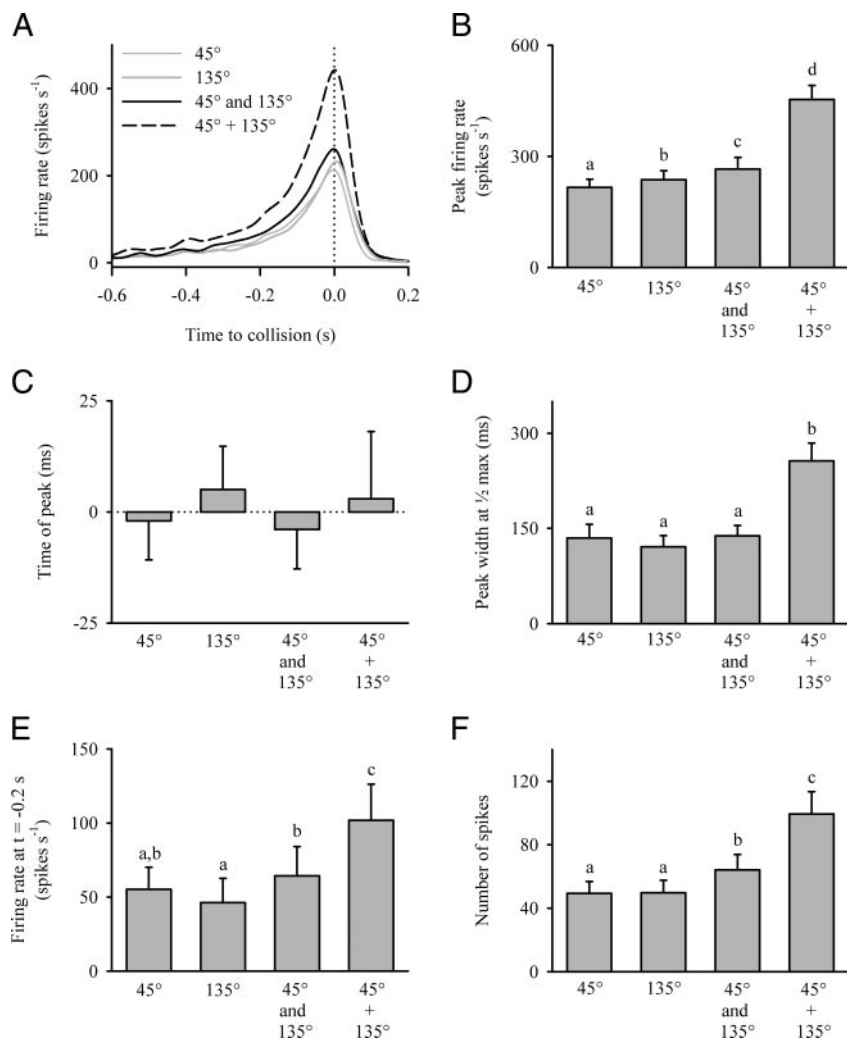


FIG. 6. Sublinear superposition of DCMD firing during simultaneous approaches of 2 looming 7 cm disks. *A*: mean plots of smoothed histograms for single approaches from 45° (thin gray line) and 135° (thick gray line) are overlaid with plots of the response to simultaneous approaches (black line) and the predicted linear sum of individual approaches (dashed line). For single objects, the peak firing rate (*B*) was highest during an approach from 135°. During simultaneous approaches, the peak rate was higher than for either single approach, whereas the timing of the peak (*C*) and the peak width at 1/2 max (*D*) were unaffected. Simultaneous approaches also produced a firing rate 200 ms before collision that was higher than for a single approach from 135° but not different from an approach from 45° (*E*). *F*: the number of spikes was the same for single approaches from either angle and significantly higher during simultaneous approaches. For all parameters except peak time, the linear sum of individual approaches was significantly greater than values obtained from simultaneous approaches whereas the timing of the peak was unaffected. Data in *B–F* represent the means \pm SD, $n = 22$. Significance assessed as in Fig. 4.

and consistently lower number of spikes during the second approach, irrespective of the approach angle (Fig. 8*J*). These data suggest that DCMD looming responses were unaffected by a previous approach 4 or 3 s earlier. A second approach presented at an azimuth of 45° and 0.106 s after the first one produced a relatively lower peak firing rate (Fig. 8*B*, gray box) that occurred later (Fig. 8*D*, gray box) compared with an initial approach from the same angle. Compared with approaches from 45°, approaches from 135° resulted in a relatively higher second peak (Fig. 8*B*, white box) that occurred earlier (Fig. 8*D*, white box). These results suggest that, for approaches at 0.106-s intervals, the second peak was strongly influenced by the presence and angle of the first approach.

To test the effects of the second approach on the response to the first occurring 0.106 s earlier, we replotted and compared the firing parameters of the first approach (0.106-s interval data) to those from single approaches from comparable angles (1st approach from 4-s interval data, Fig. 9). The second approach did not affect the peak firing rate (Fig. 9*A*), the time of the first peak relative to first collision (Fig. 9*B*), or the firing rate 200 ms before first collision (Fig. 9*D*) for either initial angle. There was, however, an effect of approach angle on the response duration ($H_3 = 17.6$, $P < 0.001$) and the number of spikes [$F(3,83) = 24.3$, $P < 0.001$]. Response duration was significantly longer for 0.106-s approach intervals (Fig. 9*C*)

due to the overlap of responses to each object. The second approach resulted in more spikes for either angle (Fig. 9*E*), and this effect was greater if the initial approach was from 45°.

Effects of approach angle on responses to overlapping approach intervals

To test the effects of the initial approach angle on firing parameters associated with the valley between peaks (0.106-s approach interval), we measured the number of spikes from the valley or first collision to 500 ms after the second collision, the time, relative to second collision, and amplitude of the valley and the peak-to-peak interval (Fig. 10). The initial approach angle had no effect on the number of spikes across either time period (Fig. 10, *A* and *B*) or the timing of the valley (Fig. 10*C*), whereas initial approaches from 45° resulted in a more pronounced valley [i.e., lower valley amplitude, Fig. 10*D* (Mann-Whitney rank sum test, $T = 304$, $P < 0.001$)] and a greater peak-to-peak interval [Fig. 10*E* (Student's *t*-test, $t_{42} = 5.8$, $P < 0.001$)].

Termination of the LGMD looming response is caused by a build-up of feedforward inhibition that is related to the size and speed of the approaching object (Gabbiani et al. 2005). It is possible that the rate of termination could be involved in constraining the valley amplitude and may be

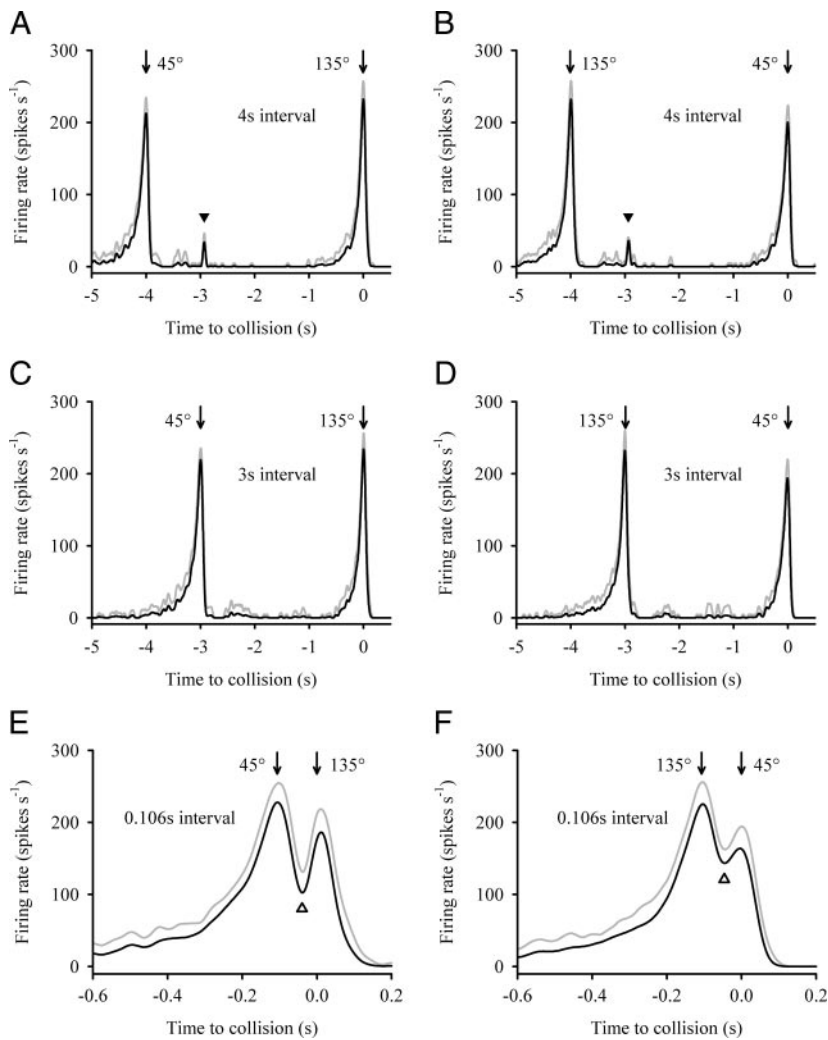


FIG. 7. DCMD responses to paired approaches at different time intervals. *A*, *C*, and *E*: responses to sequences in which the 1st approach was from 45°. and *B*, *D*, and *F*: responses to sequences in which the 1st approach was from 135°. Solid triangle, OFF response of the DCMD when the 1st object disappears, which coincides with the start of approach of the 2nd object. At this approach interval and for the 3-s interval (*C* and *D*), the response to an approach from 45° appears smaller than a response to an approach from 135°, regardless of the order of approach. During approaches at 0.106-s intervals (*E* and *F*), there are 2 distinct peaks distinguished by a valley (open arrowheads) that is more pronounced when the 1st approach is from 45°. Data represent the mean (black line, $n = 22$) and positive SD (gray line). Arrows, time of collision for each approach angle. For all plots, time 0 is the time of 2nd collision.

dependent on the approach angle. Therefore we measured the time of the last spike after the firing rate decayed to 15% of its peak value (Gabbiani et al. 2005) and calculated the time from the last expansion frame of our stimulus. This time was measured for approaches from 90° and for the first approach (4-s interval) from either 45 or 135°. We found that the last spike occurred significantly earlier for approaches from 45° [85 ± 20.0 (SD) ms] than for approaches from 135° (106 ± 20.0 ms) or 90° (117 ± 40.0 ms) and that there was no difference between the two latter conditions ($H_2 = 15.0$, $P < 0.001$, data not shown). To test for potential effects of the initial approach angle on termination of the response to the second approach (0.106-s interval), we also measured the time from the last frame of expansion (2nd approach) to the last spike using the same criteria. Termination of the second peak was not affected by the approach angle, whether the second approach was from 45° (71 ± 15.0 ms) or 135° (98 ± 26 ms). These data demonstrate that approaches from 45° terminate more quickly than approaches from 135° or 90 and further imply that objects approaching at relatively short time intervals produce DCMD firing properties that depend on the relative approach angle of each object. However, termination of the response after the second approach is not affected by the initial approach angle.

Sublinear summation of responses to overlapping approach intervals

To test whether responses to approaches 0.106 s apart result from linear superposition of individual approaches from comparable angles, we plotted the response to either angle individually as well as the linear sum with the measured response at 0.106 s intervals (Fig. 11). Because data from approaches at 0.106-s intervals were aligned to the second collision, we shifted the response of the individual approach that corresponds to the first approach angle by -0.106 s. Similar to the data for simultaneous approaches (Fig. 6) the response was sublinear for approaches at 0.106-s intervals, regardless of the initial approach angle (Fig. 11). Interestingly, even though linear superposition predicts that the first peak should be much higher (344 spikes/s) if the initial angle is 135° than if it is 45° (compare gray lines in Fig. 11, *A* and *B*) the experimental data show that firing rate of the first peak was not affected by the initial angle. Moreover the second peak was less distinct if the initial angle was 135°.

DISCUSSION

We present data from experiments designed to test whether locust DCMDs encode compound object shapes or pairs of

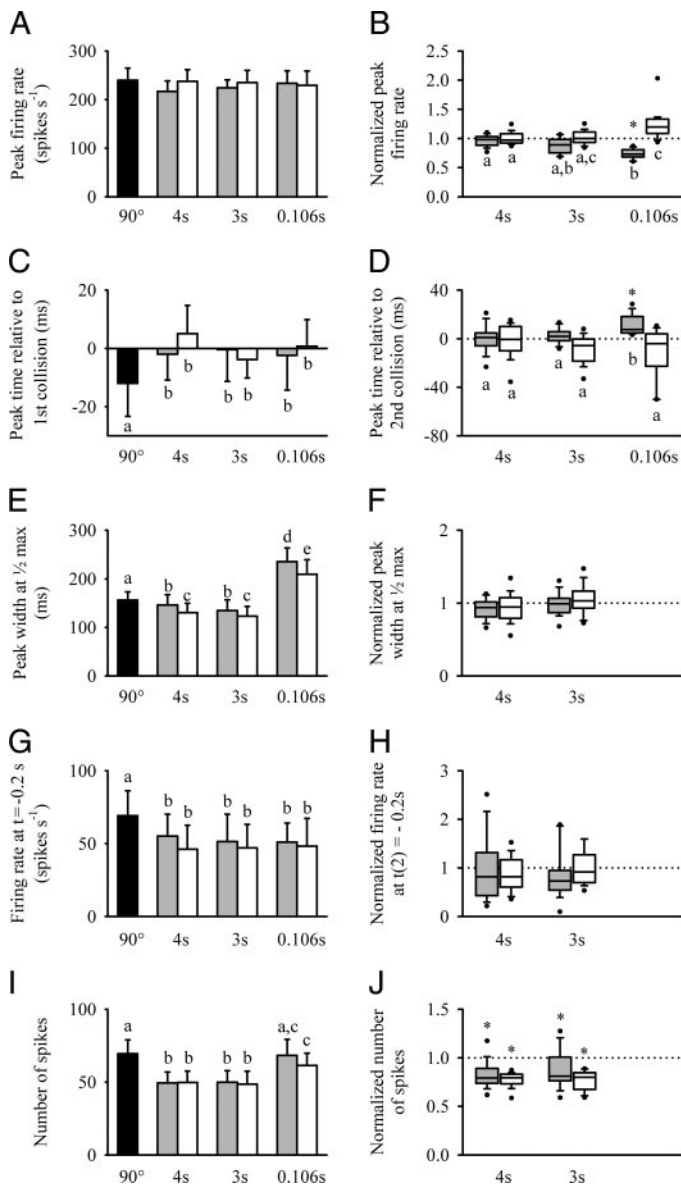


FIG. 8. Comparison of DCMD firing parameters in response to paired approaches. *A*, *C*, *E*, *G*, and *I*: data were obtained by plotting the mean \pm SD ($n = 22$) values from single approaches of a 7-cm disk from 90° (black bars) and the first approach from 45° (gray bars) or 135° (white bars). Values for responses to the second approach (*B*, *F*, *H*, and *J*) were normalized to the 1st approach except for the time of the 2nd peak relative to the 2nd collision. Boxes indicate interquartile range and median value, whiskers indicate the 5 and 95% levels and dots indicate range ($n = 22$). Gray boxes represent initial approaches from 45° and white boxes represent approaches from 135° . An asterisk indicates significant differences from the reference value (dotted lines, see text for details). Paired approaches were grouped into intervals of 4 s (4s), 3 s (3s) and 0.106 s (0.106s). Significance between normalized data assessed as in Fig. 4.

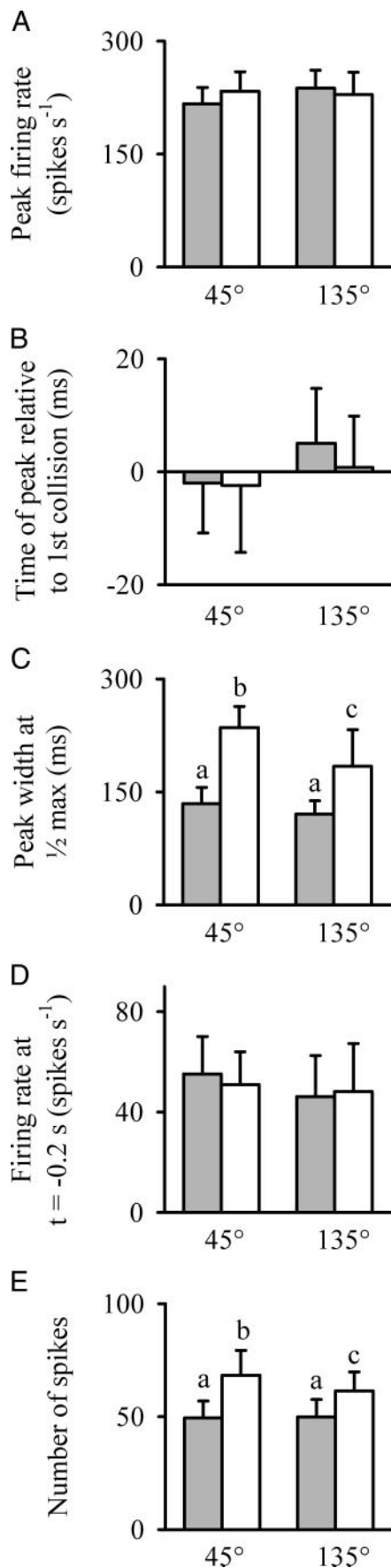
approaching objects. This is the first study to examine DCMD responses to these types of stimuli. We found that the peak firing rate during approach as well as the timing and duration of the peak were sensitive to object size but unaffected by object shape. Moreover, we found that the time of peak firing during approaches of compound objects was consistent with times predicted by a weighted value of $l/|v|$. The early phase of the DCMD response and the total number of spikes, however, were affected by the relative complexity of the approaching

object. The DCMD was sensitive to approach angles between 45° and 135° azimuth, which also produced subtle effects on responses to a second approach. Paired approaches, either simultaneous or at a short (0.106 s) interval, resulted in sublinear superposition of DCMD firing, which is consistent with sublinear processing of local inputs onto the LGMD (Krapp and Gabbiani 2005). For the short approach intervals, sublinear superposition was influenced by the relative approach angle. An interesting finding was that the DCMD was able to respond to individual approaches of paired looming objects at a behaviorally relevant time interval (0.106 s) and that the time of the second peak occurred after the second collision. These results support previous predictions (Gray 2005) that the LGMD/DCMD pathway is capable of responding to spatially and temporally complex visual stimuli.

Effects of object size and approach angle on DCMD responses

Approaches of a 7-cm disk from 90° produced a narrower, larger-amplitude peak spike rate that occurred later compared with responses to a 28-cm disk, which is consistent with previous reports on the effects of object size and speed on looming responses (Gabbiani et al. 1999, 2001; Gray 2005; Gray et al. 2001; Matheson et al. 2004; Rind 1996; Rind and Simmons 1997). The data also show that linear regression between the peak firing time and $(l/|v|)_0$ predicts that the peak occurs 20.2 ± 15.0 (SD) ms after (δ) the stimulus reached a threshold angle (θ_{thresh}) of $41.5 \pm 15.4^\circ$. Although our estimation of δ was within the range of previously reported calculations (Gabbiani et al. 1999; Gray 2005; Matheson et al. 2004), our mean value of θ_{thresh} was higher and may be due to the fact that the objects used here had a different final angular size. Given the clustering of $(l/|v|)_0$ values with the low $l/|v|$ value for a 7-cm sphere, the linear regression through the data were not particularly well defined (see Fig. 5). This may have influenced the accuracy of our estimates of δ and θ_{thresh} . However, a linear relationship between $l/|v|$ and peak firing time is well established (Gabbiani et al. 1999; Gray 2005; Matheson et al. 2004). Experiments testing a greater and more evenly spaced range of $(l/|v|)_0$ values would test directly the prediction that angular threshold computation by the LGMD is similar for approaches of simple and compound objects.

Using data from the first approach at 4- and 3-s intervals to test effects of approach angle, we found that the time of peak firing was delayed when approaches deviated from 90° (Fig. 8C). Moreover, for approach intervals of 4 and 3 s, approaches from 45° or 135° resulted in a narrower peak (Fig. 8E) and fewer spikes (Fig. 8I). A shorter approach interval (0.106 s) produced a longer duration response and a similar number of spikes compared with approaches from 90° . The longer duration is due to nonlinear summation of local inputs activated by the two approaches. For 45° approach angles, the peak firing rate, firing rate 200 ms before collision and number of spikes per trial were higher here than in an earlier report using simulated locust and bird silhouettes (Gray 2005). This difference is not unexpected given that the disks used here were defined by continuous edges that expanded uniformly during approach, whereas the different sizes and nonuniform edge expansion of the aforementioned stimuli would produce different DCMD responses. Data from approaches of compound



objects (see preceding text) predict that responses to an approaching locust or bird silhouettes would be determined by the respective $(I/|v|)_0$ value.

Invariance of peak-related firing parameters to squares approaching within an azimuth range of 30–150° (Gabbiani et al. 2001) may be due to putative position-dependent mechanisms that compensate for differences in optical density and local motion sensitivity across the equatorial visual field (Krapp and Gabbiani 2005). Our results were, therefore unexpected and may be due to differences in target shape. Gabbiani et al. (2001) found that for approaching squares, the peak firing time and number of spikes per trial were invariant for approach angles of 45, 90, and 135° (same convention as used here) but that there was a significant difference across animals in the threshold angle and peak firing time between squares and discs approaching from 90°. However, they did not test for the effects of approach angle using symmetrically expanding disks. These differences may be mediated by angle-dependent effects on response termination. LGMD responses to looming stimuli are shaped by parallel excitatory and inhibitory inputs onto two separate dendritic subfields (O'Shea and Williams 1974; Rowell et al. 1977). Excitation, mediated through a phasic lateral inhibitory network (Gabbiani et al. 2002; O'Shea and Rowell 1975b) is terminated by delayed feedforward inhibition (O'Shea and Williams 1974; Rowell et al. 1977) that defines a peak firing rate near the end of approach (Gabbiani et al. 2005; Rind 1996). A more rapid termination, as shown with our approaches from 45° (see Fig. 6A, thin line), could be due to a relatively weak or delayed wave of excitation onto LGMD inputs or, conversely, a relatively strong or advanced wave of feedforward inhibition onto subfields B and C of the dendritic tree (Hatsopoulos et al. 1995; Rowell et al. 1977). Invariance of early firing parameters across approach angles (Fig. 8G) suggest a possible combination of effects on feedforward inhibition (see following text), implying that compensation for anisotropic distributions of local retinotopic inputs and motion sensitivity (Krapp and Gabbiani 2005) may be limited for uniformly expanding looming objects. It would be interesting to test this assumption with a greater combination of object shapes and approach angles to determine if the extent of symmetry, differentiating a square and disk, during approaches that deviate from the center of the eye influences DCMD looming responses. Although the differences in peak times for objects approaching from 45 or 135° are significant and consistent (Fig. 8C), they are relatively small (~11.5 ms). Behavioral experiments that examine simultaneously the effects of approach angle on DCMD firing and collision avoidance are needed to help determine if these differences are biologically significant.

Responses to compound objects

Results from approaches of compound objects from 90° demonstrate that the peak firing rate and time as well as the

FIG. 9. Data replotted from Fig. 8 to show the influence of the 2nd object on the response to the 1st approach. Data from individual approaches (▨) are compared with the 1st approaches from the same angle of 2 objects (0.106-s interval, □). There was no effect on the peak firing rate (A), the time of the peak (B), or the firing rate 200 ms before collision (D). The duration of the response (C) was longer if the 1st approach was from 45 or 135°, and there were more spikes during a paired approach from either angle (E). Significance assessed as in Fig. 4. Data represent the means ± SD, $n = 22$.

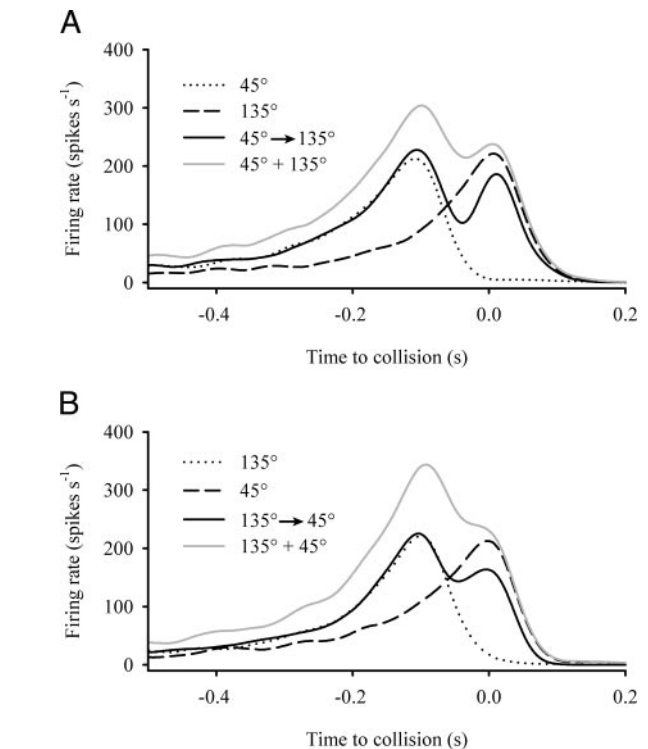
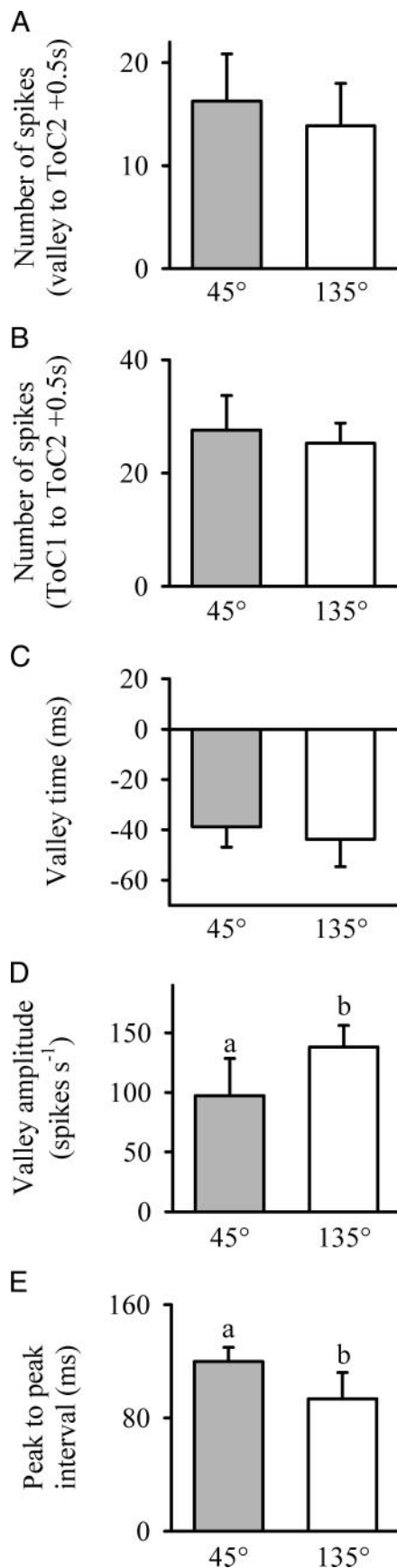


FIG. 11. Sublinear superposition of DCMD firing during approaches of 2 7-cm disks at 0.106-s intervals. The 1st approach was either from 45° (A) or 135° (B). The solid black line in each plot shows the measured instantaneous firing rate when both objects approached (separated by an arrow in the legend). These plots are overlaid on plots of individual approaches that correspond to the 1st (dotted line) and 2nd approach (dashed line) angle. The solid gray line shows the predicted linear sum of 2 independent approaches (separated by the plus sign in the legend). These data show that much of the response is shaped by the 1st approach and that the effects of the 2nd approach differ according to the 2nd approach angle. Each line represents the mean response from 22 animals.

peak duration were affected by object size but were relatively insensitive to object shape. Moreover, irrespective of the level of object complexity, the time of peak firing was consistent with values predicted by the weighted ratio, $(I/|v|)_0$ (Fig. 5). Future experiments are required to determine if this relationship is maintained across a greater range of object shapes and approach intervals. Nevertheless, these findings provide further evidence that the angular threshold computation is invariant to object shape (see Gabbiani et al. 2001), irrespective of the level of complexity. Invariance of these parameters to a 7-cm disk, HCO and VCO is likely due to a relatively small difference in the number of adjacent ommatidia being simulated during approach. Compared with a 7-cm disk, approaches of HCO and VCO would produce a relatively small increase in activation of excitatory and feedforward inhibitory pathways onto the LGMD. Moreover the long edges of the projections within the compound objects, which comprise the largest proportion of the total perimeter, subtend a final visual angle of 7°, which is

FIG. 10. DCMD firing parameters following the 1st approach (0.106-s approach interval). The number of spikes from the valley (A) or the 1st time of collision (B) through the 2nd approach was not affected by the 1st approach angle. The time of the valley relative to the 2nd time of collision (C) was also invariant. When the 1st approach was from 45° (■), the instantaneous firing rate at the time of the valley was significantly lower (D), and the peak-to-peak interval was significantly longer than when the 1st approach was from 135° (□). Significance assessed as in Fig. 4. Data represent the means \pm SD, $n = 22$.

well below the effective activation threshold for feedforward inhibition ($\sim 20^\circ$) (Gabbiani et al. 2005; Rowell et al. 1977). Therefore they would likely contribute little to a looming response. Although the short edges of these projections, i.e., the tips of the projections, would subtend a final visual angle of 109° , the edge is discontinuous across the visual field and thus would likely have a small effect on excitation through the lateral inhibitory network. Therefore it is not surprising that the peak firing rate and time as well as the response duration were insensitive to the changes in object complexity used here.

Contrary to peak-related parameters, relative object complexity did affect early phases of the DCMD response (Fig. 4D) and the total number of spikes (Fig. 4E). XCO produced values that were intermediate between a 28-cm disk and the remaining objects (7-cm disk, HCO, and VCO). Comparing between compound objects, the intermediate spike rate 200 ms before collision of XCO is due to earlier initiation and build-up of the response (compare Fig. 3, D with B and C) and a small, consistent, early peak in the firing rate. This early peak may be due to influences of the combined extensions within XCO. At 250 ms before collision, the long axes of the extensions pass through a subtense angle of 20° , potentially activating feedforward inhibition. Inhibition would likely be relatively weak, however, because the discontinuous edges would stimulate few ommatidia, producing a transient peak. Building excitation from the remaining edges would overtake this weak inhibition and the firing rate would continue to rise to a final peak, where feedforward inhibition from expansion of the central disk would ultimately terminate the response. This interpretation suggests that continually increasing $(l/v)_0$, by increasing the number of extensions, would lead to concomitant changes in the DCMD response profile that would eventually resemble responses to a 28-cm disk. Moreover, the results predict that looming asymmetrical and symmetrical objects with similar $(l/v)_0$ values should evoke similar DCMD responses. Specific influences of object shape on early phases of DCMD firing, which may be relevant for behavior (Gray 2005; Gray et al. 2001; Matheson et al. 2004), remain to be tested.

Responses to paired approaches

While paired approaches at 4- and 3-s intervals resulted in angle-dependent attenuation of the second peak firing rates, the remaining firing properties were relatively unaffected. Moreover, the maintained presence of the first object at the end of approach (i.e., 4-s interval) had little effect on the response to the second object. These findings are consistent with experiments showing that a fully habituated DCMD is able to respond to a novel looming stimulus approaching from a different angle (Gray 2005). Approaches from 45° or 135° would activate separate ommatidial arrays and thus stimulate different presynaptic inputs onto the LGMD.

A key finding of our experiments is that the DCMD was able to discriminate two closely timed objects approaching from nonoverlapping regions of the visual field and that the response was affected by the relative approach angle (Fig. 7, E and F). These findings show that the LGMD can respond to a second object during the final stages of an earlier approach when collision avoidance circuitry has been activated (Robertson and Johnson 1993). It is possible that attenuation of the second response is due to habituation effects on LGMD activation

(Gray 2005; Matheson et al. 2004; O'Shea and Rowell 1976). However, our paired objects were sufficiently spaced in the visual field that they would have stimulated different presynaptic inputs onto subfield A of the LGMD dendritic tree. It is more likely that second peak attenuation was due to nonlinear postsynaptic summation of inputs (see Gabbiani et al. 2002, 2005; Krapp and Gabbiani 2005). Angle-dependent effects on the timing of the second peak could be mediated by differences in the termination of responses to approaches from 45° and 135° (see preceding text). An earlier wave of feedforward inhibition during initial approaches from 45° would produce a more rapid decrease in the firing rate, as we found with first approaches at 4-s intervals (see RESULTS). This would cause a further reduction, i.e., deeper valley, which would then be counteracted by the next wave of excitation from the second approach. The result would be a more distinct second peak. The second peak amplitude, however, would be constrained by any remaining level of inhibition, producing equal attenuation for either combination of approach angles. Longer lasting feedforward inhibition from approaches from 135° would delay the build-up of excitation, producing a later second peak. The initial approach angle, however, did not appear to affect the second wave of feed-forward inhibition based on invariance of the time of the last spike for either second approach angle.

The relative times of excitation and feedforward inhibition could also explain why responses to the first approach are relatively unaffected by the second approach (Fig. 9). Significant activation of feedforward inhibition as the first object passes through 23° of the visual field (Gabbiani et al. 2005) occurs ~ 165 ms before the second collision. At this time, the wave of excitation from the second approach would be strongly suppressed and thus would contribute little to the firing rate. Over the next 60 ms leading to the first collision, feedforward inhibition from the first approach is even greater, further suppressing excitation from both approaches. In addition, feedforward inhibition from the second approach would begin after the first peak of the firing rate (Fig. 10E) and therefore would be unlikely to affect a response to the first approach.

Sublinear summation of multiple looming stimuli

Data from simultaneous approaches (Fig. 6) and short interval paired approaches (Fig. 11) demonstrate that summation of responses to multiple looming stimuli are strongly sublinear and that the timing of the responses is invariant. Experiments with local motion stimuli suggest that sublinear summation is governed by postsynaptic mechanisms that compensate for dendritic location of afferent inputs onto the LGMD (Krapp and Gabbiani 2005). One potential postsynaptic mechanism to explain our results may be the absolute refractory period within the LGMD spike initiating zone. Measurements from extracellularly recorded DCMD action potentials suggest that DCMD spikes last ~ 1.5 ms; this would reflect the absolute refractory period and thus limit the maximum spike rate to ~ 600 spikes/s. The maximum unfiltered firing rates for simultaneous approaches used here were between 580 and 610 spikes/s. Sublinear integration at the level of the LGMD may therefore be a consequence of the neuron's limited dynamic range. Another possible explanation of sublinear summation could involve accurate transmission of information between the LGMD and DCMD. Faithful transferral of LGMD spikes to the DCMD at

firing rates ≤ 400 spikes/s (Rind 1984) occurs via mixed electrical and chemical synapses (Killman et al. 1999; O'Shea and Williams 1974), suggesting that sublinear summation is not mediated through this specific pathway. However, further experiments would determine if fidelity across this synapse is maintained at the high spike rates reported here and elsewhere (Money et al. 2005).

Implications for flight behavior

By necessity, the experiments presented here were carried out in open-loop conditions with restrained preparations. In the natural environment, looming-induced collision avoidance behaviors (i.e., turning away from an approaching object) would modify visual input to the LGMD/DCMD pathway. In its simplest form this modification would reduce the relative approach velocity of the object, effectively terminating the loom. This assumption predicts that the DCMD response would decrease rapidly as the animal begins to turn away. Moreover, because collision avoidance involves rotation about the yaw axis, the image of the object would shift from looming to translating, which is known to evoke very different responses in the LGMD (Rind and Simmons 1992). Experiments in closed-loop conditions, where attempted steering maneuvers produce concomitant changes in the approach parameters of the object, are necessary to understand how activity in this motion-sensitive pathway relates to flight steering.

In summary, we found that DCMD responses to looming stimuli are influenced by combinations of object shape and approach angle. Moreover, the DCMD is able to respond to individual looming objects during closely timed paired approaches. Responses to paired approaches are strongly sublinear and are influenced by the relative approach angles of each object. These results are consistent with emerging studies and suggest a mechanism involving a combination of feedforward inhibition of presynaptic inputs and intrinsic properties of the LGMD. Our findings extend our understanding of responses of a looming-sensitive neuron in the context of complex visual stimuli and provide an opportunity to explore behavioral correlates as well as the underlying biophysical mechanisms through intracellular recordings of this experimentally amenable system. Such studies would test the limitations of this visual pathway within a complex visual environment and provide insights into a putative role for coordinating adaptive behaviors.

ACKNOWLEDGMENTS

A. Arkles wrote the Vision Egg code to create the visual stimuli and align the projected images with the apex of the dome screen and the center of the locust's eye. We thank R. Verspui and T.G.A. Money for providing valuable comments on an earlier version of the manuscript.

GRANTS

This work was supported by grants from the Natural Science and Engineering Research Council of Canada (NSERC) and the Canada Foundation for Innovation to J. R. Gray as well as a NSERC Undergraduate Student Research Award to B. B. Guest.

REFERENCES

Burrows M and Rowell CHF. Connections between descending visual interneurons and metathoracic motoneurons in the locust. *J Comp Physiol [A]* 85: 221–234, 1973.

- Gabbiani F, Cohen I, and Laurent G.** Time-dependent activation of feed-forward inhibition in a looming-sensitive neuron. *J Neurophysiol* 94: 2150–2161, 2005.
- Gabbiani F, Krapp HG, Koch C, and Laurent G.** Multiplicative computation in a visual neuron sensitive to looming. *Nature* 420: 320–324, 2002.
- Gabbiani F, Krapp HG, and Laurent G.** Computation of object approach by a wide-field motion-sensitive neuron. *J Neurosci* 19: 1122–1141, 1999.
- Gabbiani F, Mo CH, and Laurent G.** Invariance of angular threshold computation in a wide-field looming-sensitive neuron. *J Neurosci* 21: 314–329, 2001.
- Gibson JJ.** *The Ecological Approach to Visual Perception*. Boston, MA: Houghton Mifflin, 1979.
- Gray JR.** Habituated visual neurons in locusts remain sensitive to novel looming objects. *J Exp Biol* 208: 2515–2532, 2005.
- Gray JR, Lee J-K, and Robertson RM.** Activity of descending contralateral movement detector neurons and collision avoidance behaviour in response to head-on visual stimuli in locusts. *J Comp Physiol [A]* 187: 115–129, 2001.
- Gray JR, Pawlowski V, and Willis MA.** A method for recording behavior and multineuronal CNS activity from tethered insects flying in virtual space. *J Neurosci Methods* 120: 211–223, 2002.
- Hatsopoulos N, Gabbiani F, and Laurent G.** Elementary computation of object approach by a wide-field visual neuron. *Science* 270: 1000–1003, 1995.
- Horridge GA.** The separation of visual axes in apposition compound eyes. *Philos Trans R Soc (Lond) B* 285: 1–59, 1978.
- Judge SJ and Rind FC.** The locust DCMD, a movement-detecting neurone tightly tuned to collision trajectories. *J Exp Biol* 200: 2209–2216, 1997.
- Kayser C, Kording KP, and König P.** Processing of complex stimuli and natural scenes in the visual cortex. *Curr Opin Neurobiol* 14: 468–473, 2004.
- Killman F, Gras H, and Schürmann F-W.** Types, numbers and distribution of synapses on the dendritic tree of an identified visual interneuron in the brain of the locust. *Cell Tissue Res* 296: 645–665, 1999.
- Krapp HG and Gabbiani F.** Spatial distribution of inputs and local receptive field properties of a wide-field, looming sensitive neuron. *J Neurophysiol* 93: 2240–2253, 2005.
- Matheson T, Rogers SM, and Krapp HG.** Plasticity in the visual system is correlated with a change in lifestyle of solitary and gregarious locusts. *J Neurophysiol* 91: 1–12, 2004.
- Money TGA, Anstey ML, and Robertson RM.** Heat stress-mediated plasticity in a locust looming-sensitive visual interneuron. *J Neurophysiol* 93: 1908–1919, 2005.
- O'Shea M and Rowell CHF.** A spike transmitting electrical synapse between visual interneurons in the locust movement detector system. *J Comp Physiol* 97: 143–158, 1975a.
- O'Shea M and Rowell CHF.** Protection from habituation by lateral inhibition. *Nature* 254: 53–55, 1975b.
- O'Shea M and Rowell CHF.** The neuronal basis of a sensory analyser, the acridid movement detector system. II. response decrement, convergence, and the nature of the excitatory afferents to the fan-like dendrites of the LGMD. *J Exp Biol* 65: 289–308, 1976.
- O'Shea M and Williams JLD.** The anatomy and output connections of a locust visual interneuron: the lobula giant movement detector (LGMD) neurone. *J Comp Physiol* 91: 257–266, 1974.
- Rind FC.** A chemical synapse between two motion detecting neurons in the locust brain. *J Exp Biol* 110: 143–167, 1984.
- Rind FC.** Intracellular characterization of neurons in the locust brain signaling impending collision. *J Neurophysiol* 75: 986–995, 1996.
- Rind FC and Simmons PJ.** Orthopteran DCMD neuron: a reevaluation of responses to moving objects. I. Selective responses to approaching objects. *J Neurophysiol* 68: 1654–1666, 1992.
- Rind FC and Simmons PJ.** Signaling of object approach by the DCMD neuron of the locust. *J Neurophysiol* 77: 1029–1033, 1997.
- Robertson RM and Johnson AG.** Retinal image size triggers obstacle avoidance in flying locusts. *Naturwissenschaften* 80: 176–178, 1993.
- Robertson RM and Pearson KG.** Interneurons in the flight system of the locust: distribution, connections and resetting properties. *J Comp Neurol* 215: 33–50, 1983.
- Rowell CHF, O'Shea M, and Williams JLD.** The neuronal basis of a sensory analyser, the acridid movement detector system. IV. The preference for small field stimuli. *J Exp Biol* 68: 157–185, 1977.
- Santer RD, Simmons PJ, and Rind FC.** Gliding behaviour elicited by lateral looming stimuli in flying locusts. *J Comp Physiol [A]* 191: 61–73, 2005.

- Schlotterer GR.** Response of the locust descending movement detector neuron to rapidly approaching and withdrawing visual stimuli. *Can J Zool* 55: 1372–1376, 1977.
- Simmons PJ.** Connexions between a movement-detecting visual interneurone and flight motoneurons of a locust. *J Exp Biol* 86: 87–97, 1980.
- Simmons PJ and Rind FC.** Orthopteran DCMD neuron: a reevaluation of responses to moving objects. II. Critical cues for detecting approaching objects. *J Neurophysiol* 68: 1667–1682, 1992.
- Sun H and Frost BJ.** Computation of different optical variables of looming objects in pigeon nucleus rotundus neurons. *Nat Neurosci* 1: 296–303, 1998.
- Waloff Z.** Orientation of flying locusts, *Schistocerca gregaria* (Forsk.), in migrating swarms. *Bull Ent Res* 62: 1–72, 1972.
- Wicklein M and Strausfeld NJ.** Organization and significance of neurons that detect change of visual depth in the hawk moth *Manduca sexta*. *J Comp Neurol* 424: 356–376, 2000.
- Wilson M.** Angular sensitivity of light and dark adapted locust retinula cells. *J Comp Physiol* 97: 323–328, 1975.
- Zoccolan D, Cox DD, and DiCarlo JJ.** Multiple object response normalization in monkey inferotemporal cortex. *J Neurosci* 25: 8150–8164, 2005.